

RESEARCH ARTICLE

Lateral load performance of a reinforced concrete frame with pultruded GFRP box braces

Tuna Ulger¹, Muhammet Karabulut¹, Necati Mert²

- ¹ Zonguldak Bulent Ecevit University, Department of Civil Engineering, Zonguldak, Türkiye
- ² Sakarya University, Department of Civil Engineering, Sakarya, Türkiye

Article History

Received 17 January 2022 Accepted 4 March 2022

Keywords

Pultruded GFRP
Lateral load capacity
Reinforced concrete frame
Pushover analysis
Box brace
Buckling

Abstract

Reinforced concrete buildings, which constitute most of the building stock in Turkey, should be examined in terms of earthquake resistance. Many studies have been carried out to increase the seismic resistance of reinforced concrete (RC) structures against earthquakes. In this study, a single-story, single-span RC frame stiffened with chevron steel braces was chosen as a reference frame and laterally loaded to failure. In the first step, the experimentally obtained static lateral loaddeflection curve was verified by non-linear finite element (FE) analysis. Then, the uniaxial tensile properties of the selected glass fiber reinforced polymer (GFRP) materials were verified using FE analysis with the results found in the literature. In the second step, three different GFRP box braces with different axial stiffnesses were investigated and the results were compared with those of the steel chevron braces. Finally, the lateral load performance and expected buckling failure of the GFRP box braces in an RC moment frame have been presented and discussed in this study. Considering the lightweight of the GFRP sections, the lateral load capacity of the RC frame with GFRP braces was improved as much as the steel braces, and the maximum gain was about 47% more when the equal axial stiffness of steel brace was provided to GFRP brace. Ductility and story drift of the considered braced moment frames are presented.

1. Introduction

Many earthquakes occur in the world, especially in Turkey. These earthquakes cause the loss of many human lives and the destruction or damage of buildings. When the existing reinforced concrete (RC) buildings in our country are examined in terms of earthquake safety, it is known that many structures are insufficient. Many different techniques have been applied to the reinforcement of reinforced concrete structures and innovative studies on this subject are still ongoing. Existing reinforced concrete structures with improper concrete strength and reinforcements can be strengthened by considering structural subcomponents. Column jacketing or fiber polymer bonding applications can be listed among the subcomponent strengthening methods. Adding a shear wall to the structure, reinforcement of infill walls, or brace applications can be considered to strengthen the load resisting system. Recently, strengthening methods have been investigated using polymer composites. For example, laminates, sheets, bars, and pultruded sections are common forms of composites in strengthening studies. Rasheed et. al. [1] investigated the use of bonded biaxial CFRP sheets in the flexural strengthening of the T-section concrete girders. The effectiveness of anchorage on the

longitudinal CFRP sheets was investigated by bonding U-shaped GFRPs to the web of the T section. It was shown that the FRP anchorage provided higher load capacities and fewer deflections compared to the unanchored longitudinal sheets. Hu et. al [2] focused on the flexural strengthening of reinforced concrete beam bonding FRP composites using nonlinear finite element analysis. The relation between the length of the beams, fiber angles, and FRP locations was investigated. Aksoylu and Kara [3] investigated the lateral load performance of the RC moment frames with high-strength diagonal precast panels. The ultimate load capacity, lateral stiffness, and energy absorption capacity of the un-strengthened frames were increased approximately 4, 12, and 4 times by including the panels. Cruz et. al. [4] investigated optimized ductility enhancement of the RC framed buildings. It was reported that FRP wrapping was found more efficient than steel jacketing for column strengthening, and braces provided the highest ductility enhancement in buildings. In a similar study, Castaldo et. al. [5] focused on the seismic performance of an existing RC structure retrofitted with buckling restrained braces. Mahdavipour et. al. [6] utilized externally bonded FRPs on RC buildings for retrofitting with externally bonded FRPs. It was concluded that variation of structural parameters and the use of different retrofitting schemes had significant effects on the failure mode of the frames. Ferracuti et. al. [7] investigated RC frame structures retrofitted by wrapping CFRP sheets with numerical models under axial and cyclic loading. Pushover curves of those retrofitted frames against lateral loads were presented with ductility improvements. Similar cyclic loading was applied on rectangular columns after bonding hybrid CFRP and GFRP sheets at their plastic hinge locations [8]. A different number of FRP layers and lengths were studied experimentally, and increased ductility and reduced displacement capacities were reported after different strengthening considerations. Concrete beams with web openings strengthened in shear by bonding FRP sections have been studied by Kareem [9] and ultimate load capacity and stiffness enhancements were reported, and corresponding failure modes were presented. Erdem et. al. [10] investigated strengthening techniques for RC frames including special wall-frame connection using CFRP strips and dowels. The effectiveness of the proposed method highly depends on the dowel connections which is true for other mechanical connections in strengthening applications [10,11]. Braced systems for strengthening the RC frames were investigated to enhance the lateral load resisting capacities and their effectiveness was reported in the literature [11-13]. Pultruded GFRP stiffeners were investigated on buckling prone steel webs [14], and shear strength capacity was increased up to %54. This showed that the pultruded sections can be utilized for RC structures.

In this study, pultruded GFRP box sections were planned to be utilized as brace members in RC structures. One of the RC frames which was experimentally tested [11] was selected for the reference study. The experimental study was first verified with numerical models. Experimentally obtained mechanical properties of the GFRP sections [15] were included in finite element analysis for failure detections and load capacity calculations. The performance of GFRP chevron braces was compared with steel braces in terms of load capacities, stiffness, and failure mechanisms.

2. Materials and test methods

2.1. RC frame models

One of the RC frame test set-ups from the literature was chosen as a reference frame model which was obtained from 1/3 of a full-size RC frame [11]. The adopted reference frame is a single-span and -story frame with 15×20 cm and 15×15 cm beam and column cross-sections, respectively. The beam section was reinforced with $4\phi10$ mm longitudinal bars and confined with $\phi5$ mm stirrups at 10 cm intervals. Column sections have $5\phi10$ mm longitudinal reinforcements and are transversely confined identical to the beam section. The foundation of the frame was designated relatively wider, deeper, and stiffer than the RC frame, and the technical drawing of the RC frame was provided in Fig 1. The same scaled RC frame was laterally

strengthened by IPE100 steel chevron braces and was experimentally tested to get increased load capacity of the RC frame with chevron braces.

In FE models of the RC frames, a strong beam-weak column design was made in the beam-column junctions to reflect the general situation of the reinforced concrete structure which needs to be addressed for old detailed framed structures in Turkey. Additionally, proper tie spacings at columns` confined regions and beam-column joints were not provided in those buildings [16]. The FE model of the reference RC concrete frame is given in Fig 2a and the details of the beam, column, and foundation sections created in SAP2000 are shown in Fig. 2b. Displacement controlled experimental test protocol was applied in the reference study [11], and the same protocol was included in FE model simulations.

2.2. Concrete

The nominal compressive strength of C20/25 was selected for the experiments, and the ultimate compressive strength of those concrete samples was calculated at 31.94 MPa from the standard cube samples [11]. It was calculated that the ultimate compressive strength of the concrete was 25.5 MPa after correcting the cube sample results to the cylindrical sample values. Steel reinforcement was grade S420 steel with a yield strength of 420 MPa. Confined Non-linear Mander concrete material model and elastic – perfectly plastic Park steel material model were defined in the FE models. The stress-strain diagram of the materials in the experimental tests is shown in Fig. 3a and 3b, respectively.

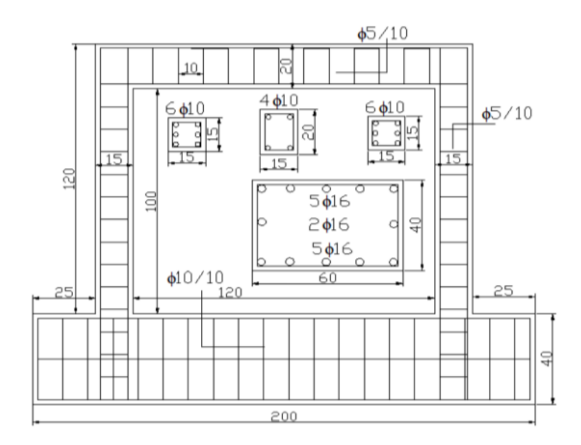


Fig. 1. Geometric and reinforcement detail of the reinforced concrete frame [13] (cm unit)

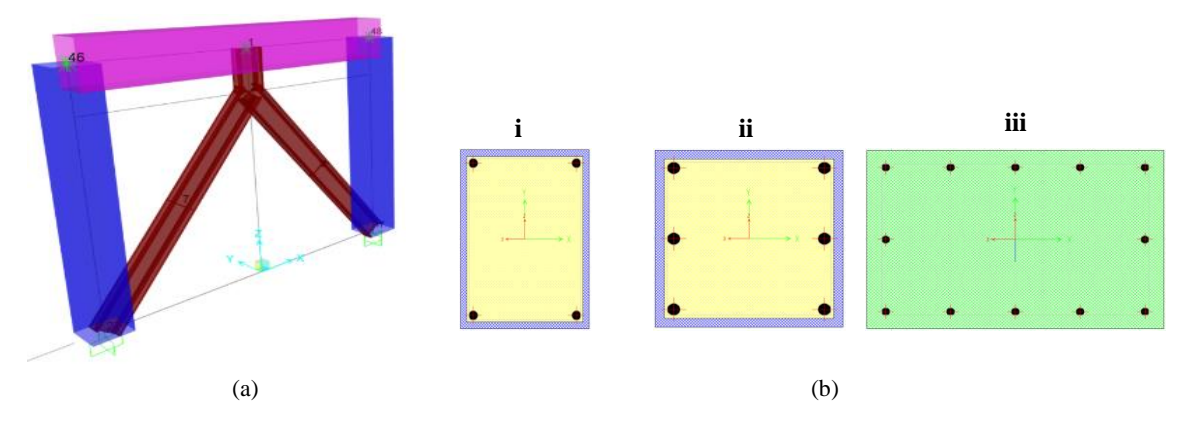


Fig. 2. Reference RC frame and cross-sections: (a) 3D FE Model with IPE100 profile, (b) Beam (i), column (ii) and foundation (iii) sections

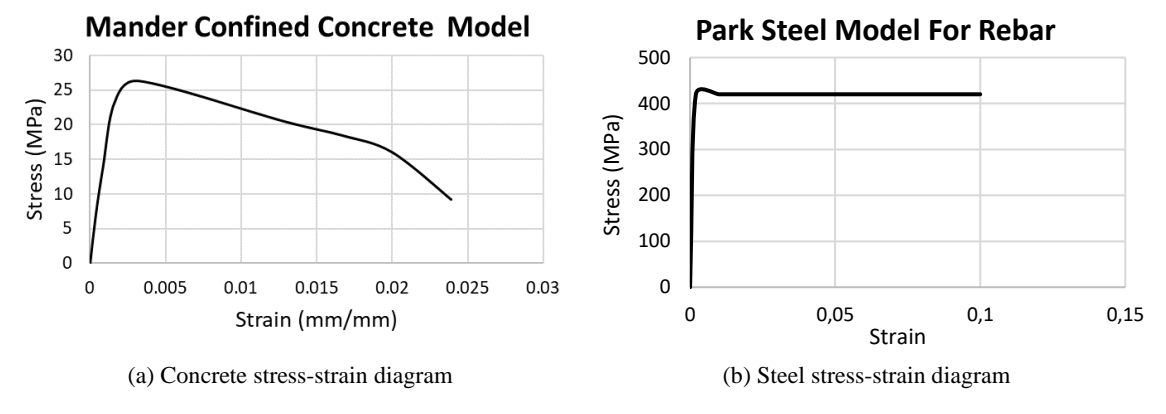


Fig. 3. Non-linear material properties in FE models

2.3. GFRP coupons and sections

Experimentally obtained mechanical properties of the GFRP coupons were assigned to the GFRP box sections in the FE models. Uniaxial tensile test coupon samples in accordance with the relevant standards [17-19] and test conditions were prepared and tested [15]. After the tensile tests were performed, the tensile properties and modulus of elasticity of the GFRP composite material were calculated following the work done by Aydın and Sarıbıyık [15]. A total of 10 test specimens of 25x250x4 mm size were used for the tensile test parallel to the fiber direction. The average experimental test results were summarized in Table 1 for the GFRP coupons. To verify the tensile strength and failure of GFRP material, a sample coupon model (25x250x4 mm) was created and tested under nonlinear uniaxial tension tests in the FE models. It was ensured that the desired rapture of the GFRP material could be captured as in the experimental tension tests by assigning an axial plastic hinge at the mid-height of the coupons. However, slight softening behavior was included in FE models to eliminate the non-convergence problems. The experimental and verified FE model stress-strain curves of the GFRP coupons are shown in Fig. 4. As a result, one can see in Fig. 4 that experimental and numerical results are very consistent and accurate by considering the engineering error limits. Therefore, the mechanical behavior of the GFRP sections was simulated by axial hinge definition in FE models if the sections do not buckle. On the other hand, if the GFRP section buckles, the axial hinge will not develop, and it will not reach the ultimate axial load capacity. It should be stated that the compression and tension properties of the GFRP sections are assumed equal in FE models.

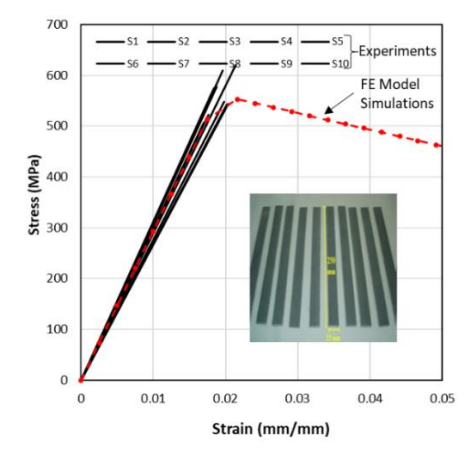


Fig. 4. Numerically validated uniaxial tensile test of GFRP coupons [15]

Table 1. Assigned concrete [11] and GFRP [15] material properties in FE models	

Material	Elastic modulus (MPa)	Poisson ratio (μ)	Ultimate fracture/compressive strength (MPa)
GFRP	29334	0.34	561
Concrete	27000	0.30	25.5

In this study, the RC frame was reinforced with three different GFRP box sections and their geometric properties are shown in Fig. 5. The relative axial stiffness ratio of the selected GFRP box sections to the steel IPE 100 was 1.0, 0.5, and 0.2 for the numerical study. The effectiveness of the GFRP box sections within the RC moment frame was investigated, and their dimensional and mechanical properties that were assigned in FE models are given in Table 2. Initial imperfections of all the braces were accounted for in FE models with a unit (1 mm) out-off plane deflection at the middle of each brace. Therefore, geometric and material nonlinearities of the GFRP braces were included within the possible failure of the considered moment frames.

3. Results and Discussions

3.1. FE models with experimental tests

Load deflection curves of the bare reinforced concrete frame with and without steel braces were obtained from the numerical analysis, and their experimentally obtained load-deflection curves were plotted together in Fig. 6a. The ultimate load capacity of the bare frame was obtained at 47.1 kN, and that capacity was 47.0 kN with the developed FE model. Therefore, a 0.21% error was calculated between the experiment and FE model results in a bare RC frame. On the other hand, the full load capacity of the steel braced frame was not reached due to the premature failure (bolt slip) at the column base during the experiment [11]. The shear strength of the column and beam sections was estimated using Eq. (1) in TS500, and the column and beam have approximated 138 and 165 kN shear load capacities, respectively. Therefore, these unexpected failures were not included in this study, however, the possible shear failures are included in the capacity estimation of the FE model of RC frames by assigning the shear hinges. Therefore, these two experiments were validated with FE models and provided acceptable accuracy for the prediction of the lateral load capacity and displacement of the RC frame models. The column base cracks were observed in the reference study at failure, and the formation of the plastic hinges due to shear and moments were similarly captured in FE models as shown in Fig. 6b.

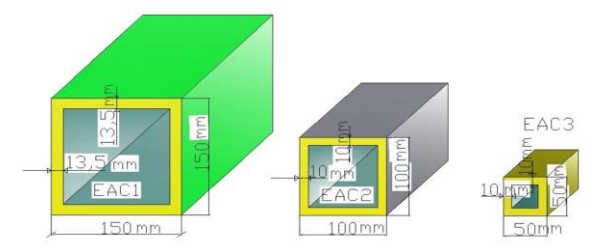


Fig. 5. GFRP box brace cross-sections

Table 2. GFRP Box section properties [15]

Brace section	Dimensions (mm)	Area (mm²)	Elastic modulus (MPa)	Yield/rupture strain (mm/mm)	EAGFRP/EAIPE100
EAS	IPE 100	1013	200000	0.002	1
EAC1	150×150×13.5	7371			1
EAC2	100×100×10	3600	29333	0.02	0.5
EAC3	50×50×10	1600			0.2

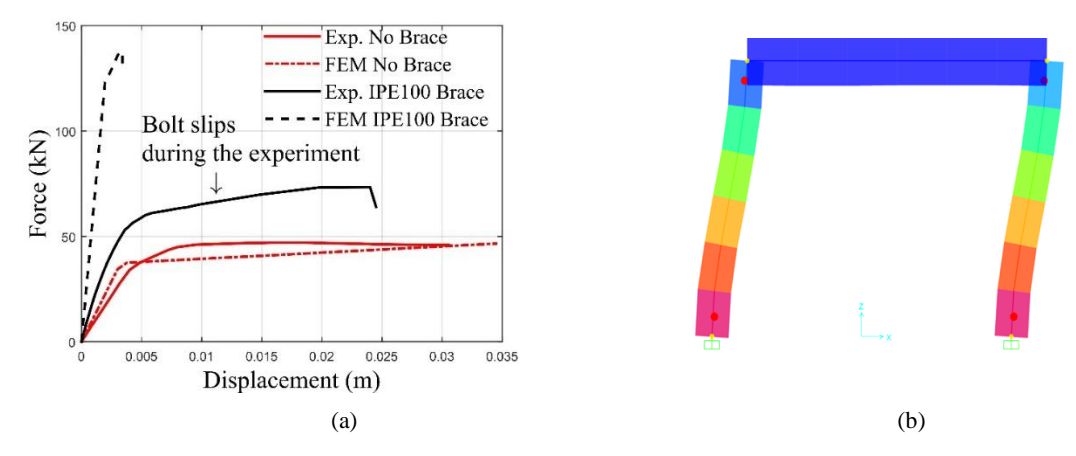


Fig. 6. (a) FE model verification of the experiments [11], (b) Plastic hinge formations

3.2. GFRP box braces

The result of the FE model analysis of all the RC moment frames with the chevron GFRP box braces is presented in this part of the study. The lateral load-deflection curve of the bare RF moment frame was showed the 47.1 kN ultimate load capacity, and the frame started to yield at about 0.003 m lateral deflection. The inclusion of chevron IPE100 steel braces was increased the load capacity of the EAS frame up to 138 kN, and the initial stiffness of the bare RC frame was increased by about 342% with EAS braces. The steel braces did not buckle during the experiment and FE model analysis. The counterpart GFRP box brace with the same axial stiffness of the IPE100 section, EAC1, was included in the RC frame model, and the maximum load capacity was increased up to 165.8 kN as shown in Fig. 7, which is 20% more than that of EAS braces. The hinge formation showed that multiple plastic hinges were formed at the columns and beams. In the meantime, the critical buckling load capacities were calculated per brace using the Euler's buckling formal given in Eq. 2 [20] and FE model nonlinear buckling analysis. The critical buckling load capacities of the GFRP Box sections were tabulated in Table 3. The smallest buckling load capacity of the EAC1 brace was calculated at 4925 kN which showed that the buckling of the brace was not a controlling failure in the RC frame.

In the second case, EAC2 braces were assigned to the reference RC frame. The ultimate load capacity was calculated at 136.9 kN which was almost identical to the EAS braced RC frame`. However, a 50% reduction in the axial stiffness of the GFRP braces caused about 33% of the initial stiffness reduction. In Fig. 7, the load-deflection curve of EAC2 braces did not axially yield or buckled until the plastic hinges formed at the RC frame.

In the last case, when the axial stiffness ratio of the EAC3 braces was reduced by 0.2 of the steel braces`, EAS, the load capacity was reached up to 108.2 kN which was less than the load capacity of the RC frame with EAS braces. The EAC3 braces were the slenderest section among the other GFRP box braces. During the FE analysis, it was found that the critical buckling load capacity of 103 kN was also reached at 0.0093 mm lateral deflection. The load-deflection history of the EAC3 braces is given in Fig. 7.

On the other hand, the ductility of the considered strengthening methods was evaluated over the area under the load-displacement curves (Fig 7) and given in Table 4. This reduction reached a maximum, of 80% of the bare moment frame when the EAC1 brace was assigned. On the other hand, story drift was reduced by about 93% against bare moment frame and 34% against steel braced EAS moment frame with the EAC1 braces. Therefore, the proposed braced moment frames suffer due to reduced ductility, however, secondary moments due to story drifts become less destructive in braced moment frames.

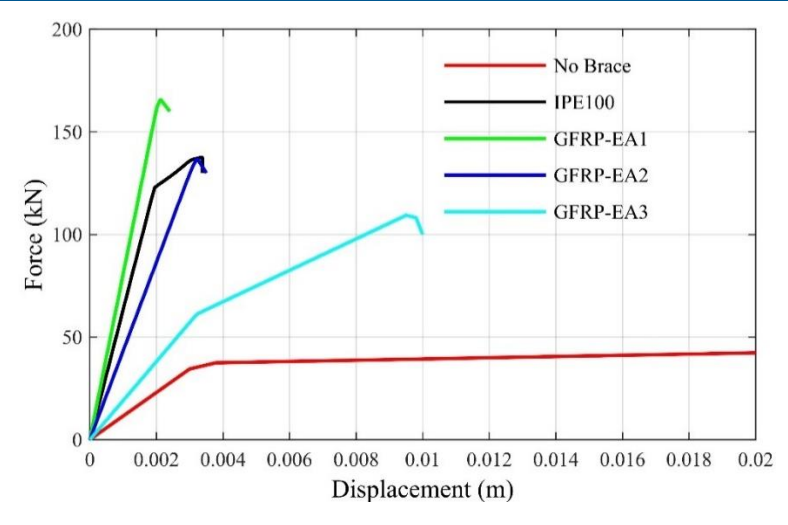


Fig. 7. Load deflection curves of braced RC moment frames from FE analysis

$$V_r = V_c + V_w$$

$$V_c = \mu_c \times f_{ctd} \times b \times d$$

$$V_w = \mu_s \times F_{vw} \times {}^{A_{sw}}/_{S} \times d$$
(1)

$$P_{cr} = \frac{\pi^2 EI}{L^2} \tag{2}$$

The notations in Eqs. 1 and 2 can be listed as: V_r = Total shear resistance, V_c = Shear resistance due to concrete, V_w = Shear resistance due to steel reinforcement, μ_c = 1 reduction factor, μ_s = 1.15 steel overstrength factor, f_{ctd} = tension strength of concrete, F_{yw} = reinforcement yield strength, A_{sw} = reinforcement area, b and d = section dimensions, P_{cr} = critical buckling load, EI = flexural rigidity, L = length of the member.

3.3. Plastic hinge formations at failure

The failure of the RC frame and braces were followed in this section by the plastic hinge definitions. These hinges show the final stage of the failed section as shown in Fig. 8, and they are important to control the failure mechanism of the laterally stiffened frames. The EAS steel brace showed axial yielding in the compression brace as shown in Fig. 8a and buckling of that brace was expected to occur at about 122 kN as shown in Fig. 7. The EAC1 and EAC2 braces did not axially yield and buckle during the lateral loading and the deflected shape of the frame at the final loading stages were shown in Fig. 8b and Fig. 8c, respectively. The plastic hinge did not develop in both GFRP braces. Finally, the slender GFRP braces were yielded and buckled at about 62.5 kN during the lateral loading, and the plastic hinge formations of EAC3 braces can be seen in Fig. 8d. EAC3 braces allowed maximum lateral deflection among the braced RC frames which also caused the multiple plastic hinge formations on the beam and column elements of the RF frame. On the other frames plastic hinges in the RC frames were not fully developed at their peak loads as shown in Fig. 8a to Fig. 8c. The same conclusion can be drawn for these braces from Fig. 7 that the numerical instability problems caused the load drops after their peak load capacities were reached. At the same time, it was assumed that column and beams have reached their theoretically calculated shear strengths until these peak loads were achieved during the lateral loadings. Nevertheless, the lateral load capacities and corresponding failure locations on the RC beams and braces can be seen in Fig. 8.

Table 3.	Critical	buckling	loads of	GFRP 1	box sections
----------	----------	----------	----------	--------	--------------

Section name	Numeric buckling load (kN)	Euler buckling load (kN)
EAC1	4925	5287
EAC2	1075	1125
EAC3	103.4	103.7

Table 4. Failure loads, lateral drifts, and ductility of the braced frames using FE analysis

Section name	Failure load (kN)	Lateral drift at failure (mm)	Area under the load-deflection curves (kN-mm)
No Brace	47.1	30.0	869
EAS	138.0	3.2	218
EAC1	165.8	2.1	174
EAC2	136.9	3.1	212
EAC3	108.2	9.3	728

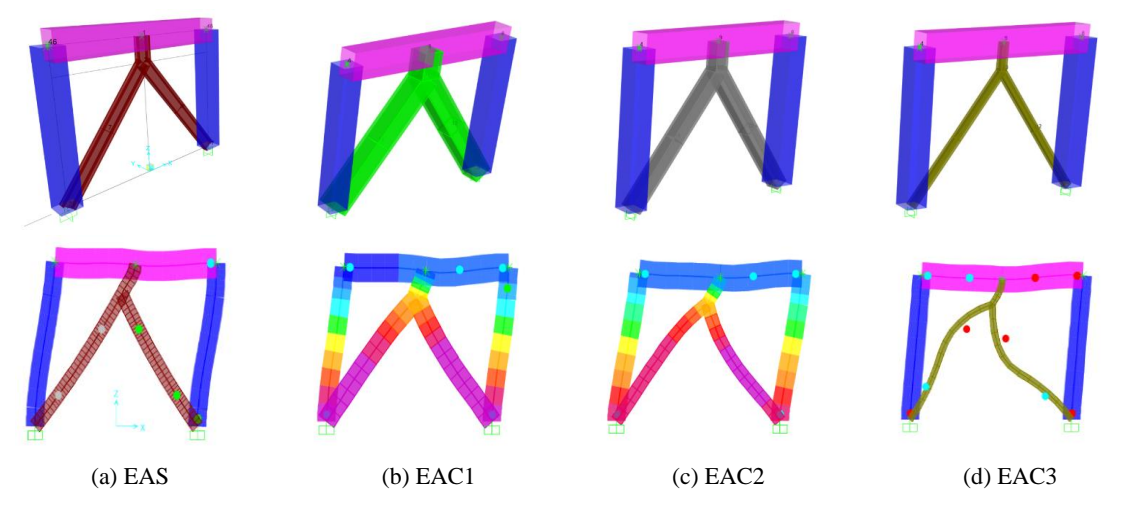


Fig. 8 Different type brace configurations in a RC frame with final hinge formations

4. Conclusions

Chevron-type brace configuration inside a reinforced concrete moment frame was investigated in this study. The experimental results of the moment frame with and without steel braces were verified in FE models. The alternative use of three different GFRP box braces was utilized inside the verified FE moment frames and, their expected ultimate load capacities and corresponding lateral deflections were presented and compared to the structural performance of the steel braces. The axial stiffness reduction and out-off plane buckling of the GFRP braces were included in the possible failure of the considered moment frames.

When the equally axial stiffness of IPE100 braces was provided to the GFRP box braces, lateral load capacity was increased without the possibility of buckling. When half of that axial stiffness was provided to the GFRP box braces, the load capacity was obtained close to the load capacity of GFRP box braces however, the initial stiffness in the linear loading phase was obtained slightly less than the IPE100 braces`. Failure of the GFRP box braces did not occur until the peak load. The slender GFRP box section was more vulnerable to buckling failure, and it occurred before the plastic hinges developed in the moment frames. The slender

section with 20% axial stiffness of the IPE100 steel braces showed the least lateral performance among the GFRP braces.

In terms of energy dissipation capacities, the total ductility of the bare moment frame was reduced by including the braces. On the other hand, the lateral drift was controlled with the braced moment frames. Therefore, braces performed well to inhibit the sway action of the moment frames.

Considering the advanced mechanical properties of GFRP sections, such as being a light material and reducing the total weight of the structure, resistant to corrosion, and more economical with the advanced production methods, GFRP sections can be used as the main structural lateral resistant component in a full-size structure. Further study can investigate the effectiveness of the GFRP braces in multi-story and multi-opening moment framed structures. In the same scope, the connectivity of the GFRP section to the concrete needs to be addressed, and the stiffness losses due to connection details can be specifically included in future studies.

Declaration of conflicting interests

The author(s) declared no potential conflicts of interest with respect to the research, authorship, and/or publication of this article.

References

- [1] Rasheed HA, Zaki MA, Foerster AS (2022) Efficient bidirectional U-wrap system to anchor CFRP sheets bonded to reinforced concrete T-girders. Structures. 38:226–236.
- [2] Hu HT, Lin FM, Jan YY (2004) Nonlinear finite element analysis of reinforced concrete beams strengthened by fiber-reinforced plastics. Composite Structures 63:271–281.
- [3] Aksoylu C, Kara N, (2020) Strengthening of RC frames by using high strength diagonal precast panels. Journal of Building Engineering 31: 101338.
- [4] Cruz MVRG, Esteban AM, Neyra PD (2021) Optimal ductility enhancement of RC framed buildings considering different non-invasive retrofitting techniques. Engineering Structures 242:112572.
- [5] Castaldo P, Tubaldi E, Selvi F, Gioiella L (2021) Seismic performance of an existing RC structure retrofitted with buckling restrained braces. Journal of Building Engineering 33:101688.
- [6] Mahdavipour MA, Eslami A, Jehel P (2020) Seismic evaluation of ordinary RC buildings retrofitted with externally bonded FRPs using a reliability-based approach. Composite Structures 232: 11567.
- [7] Ferracuti B, Savoia M, Zucconi M (2020) RC frame structures retrofitted by FRP-wrapping: A model for columns under axial loading and cyclic bending. Engineering Structures 207:110243.
- [8] Shin DH, Kim HJ (2020) Cyclic response of rectangular RC columns retrofitted by hybrid FRP sheets. Structures 28:697-712.
- [9] Kareem AHA (2014) Shear strengthening of reinforced concrete beams with rectangular web openings by FRP Composites. Advances in Concrete Construction 2(4):281-300.
- [10] Erdem I, Akyuz U, Ersoy U, Ozcebe G (2006) An experimental study on two different strengthening techniques for RC frames. Engineering Structures 28:1843-1851.
- [11] Ince G, Tekeli H, Ince HH, Ocal C, Mercan K, Ulutaş H (2015) Reinforcement of RC frames with eccentrically braced vertical links. In Proceedings of IBEES2015: International Burdur Earthquake & Environment Symposium. Burdur, Turkey
- [12] Ozcelik R, Binici B, Kurç O (2012) Pseudo dynamic testing of an RC frame retrofitted with chevron braces. Journal of Earthquake Engineering 16:515-539.
- [13] Karalis AA, Stylianidisa KC (2013) Experimental investigation of existing R/C frames strengthened by high dissipation steel link elements. Earthquakes and Structures 5(2):143-160.
- [14] Ulger T, Okeil AM (2017) Strengthening by stiffening: fiber-reinforced plastic configuration effects on behavior of shear-deficient steel beams. Journal of Composites in Construction 21:04017011.
- [15] Aydın F, Sarıbıyık M (2013) Investigation of flexural behaviors of hybrid beams formed with GFRP box section and concrete. Construction and Building Materials. 41:563–569.

[16] Yılmaz EE, Uzun M, Cogurcu MT (2018) Strengthening the reinforced concrete frames and enhancing the earthquake performance. Journal of Selcuk-Technic 17(3)-2018.

- [17] ASTM D 3039 M-08 (2007) Standard test method for tensile properties of polymer matrix composite materials. ASTM (American Society for Testing and Materials).
- [18] TS EN ISO 527-4. (2007) Plâstikler–Çekme Özelliklerinin Tayini–Bölüm 4: Izotropik ve Ortotropik Elyaf Takviyeli Plâstik Kompozitler İçin Deney Standartları. Türk Standartları Enstitüsü.
- [19] TS EN ISO 527-5. (2010) Plâstikler–Çekme Özelliklerinin Tayini–Bölüm 5: Tek Yönlü Elyaf Takviyeli Plâstik Kompozitler Için Deney Standartları. Türk Standartları Enstitüsü.
- [20] Yoo CH, Lee SC (2011) Stability of Structures Principles and Applications, First Edition. Elsevier Inc.